

Evidence for CP Violation in Time-Integrated $D^0 \rightarrow h^- h^+$ Decay Rates

R. Aaij *et al.**

(LHCb Collaboration)

(Received 6 December 2011; published 12 March 2012; publisher error corrected 12 March 2012)

A search for time-integrated CP violation in $D^0 \rightarrow h^- h^+$ ($h = K, \pi$) decays is presented using 0.62 fb^{-1} of data collected by LHCb in 2011. The flavor of the charm meson is determined by the charge of the slow pion in the $D^{*+} \rightarrow D^0 \pi^+$ and $D^{*-} \rightarrow \bar{D}^0 \pi^-$ decay chains. The difference in CP asymmetry between $D^0 \rightarrow K^- K^+$ and $D^0 \rightarrow \pi^- \pi^+$, $\Delta A_{CP} \equiv A_{CP}(K^- K^+) - A_{CP}(\pi^- \pi^+)$, is measured to be $[-0.82 \pm 0.21(\text{stat}) \pm 0.11(\text{syst})]\%$. This differs from the hypothesis of CP conservation by 3.5 standard deviations.

DOI: 10.1103/PhysRevLett.108.111602

PACS numbers: 13.25.Ft, 11.30.Er, 13.85.Ni

The charm sector is a promising place to probe for the effects of physics beyond the standard model (SM). There has been a resurgence of interest in the past few years since evidence for D^0 mixing was first seen [1,2]. Mixing is now well established [3] at a level which is consistent with, but at the upper end of, SM expectations [4]. By contrast, no evidence for CP violation in charm decays has yet been found.

The time-dependent CP asymmetry $A_{CP}(f; t)$ for D^0 decays to a CP eigenstate f (with $f = \bar{f}$) is defined as

$$A_{CP}(f; t) \equiv \frac{\Gamma(D^0(t) \rightarrow f) - \Gamma(\bar{D}^0(t) \rightarrow f)}{\Gamma(D^0(t) \rightarrow f) + \Gamma(\bar{D}^0(t) \rightarrow f)}, \quad (1)$$

where Γ is the decay rate for the process indicated. In general $A_{CP}(f; t)$ depends on f . For $f = K^- K^+$ and $f = \pi^- \pi^+$, $A_{CP}(f; t)$ can be expressed in terms of two contributions: a direct component associated with CP violation in the decay amplitudes, and an indirect component associated with CP violation in the mixing or in the interference between mixing and decay. In the limit of U -spin symmetry, the direct component is equal in magnitude and opposite in sign for $K^- K^+$ and $\pi^- \pi^+$, though the size of U -spin breaking effects remains to be quantified precisely [5]. The magnitudes of CP asymmetries in decays to these final states are expected to be small in the SM [5–8], with predictions of up to $\mathcal{O}(10^{-3})$. However, beyond the SM the rate of CP violation could be enhanced [5,9].

The asymmetry $A_{CP}(f; t)$ may be written to first order as [10,11]

$$A_{CP}(f; t) = a_{CP}^{\text{dir}}(f) + \frac{t}{\tau} a_{CP}^{\text{ind}}, \quad (2)$$

*Full author list given at the end of the article.

Published by the American Physical Society under the terms of the [Creative Commons Attribution 3.0 License](https://creativecommons.org/licenses/by/3.0/). Further distribution of this work must maintain attribution to the author(s) and the published article's title, journal citation, and DOI.

where $a_{CP}^{\text{dir}}(f)$ is the direct CP asymmetry, τ is the D^0 lifetime, and a_{CP}^{ind} is the indirect CP asymmetry. To a good approximation this latter quantity is universal [5,12]. The time-integrated asymmetry measured by an experiment, $A_{CP}(f)$, depends upon the time acceptance of that experiment. It can be written as

$$A_{CP}(f) = a_{CP}^{\text{dir}}(f) + \frac{\langle t \rangle}{\tau} a_{CP}^{\text{ind}}, \quad (3)$$

where $\langle t \rangle$ is the average decay time in the reconstructed sample. Denoting by Δ the differences between quantities for $D^0 \rightarrow K^- K^+$ and $D^0 \rightarrow \pi^- \pi^+$ it is then possible to write

$$\begin{aligned} \Delta A_{CP} &\equiv A_{CP}(K^- K^+) - A_{CP}(\pi^- \pi^+) \\ &= [a_{CP}^{\text{dir}}(K^- K^+) - a_{CP}^{\text{dir}}(\pi^- \pi^+)] + \frac{\Delta \langle t \rangle}{\tau} a_{CP}^{\text{ind}}. \end{aligned} \quad (4)$$

In the limit that $\Delta \langle t \rangle$ vanishes, ΔA_{CP} is equal to the difference in the direct CP asymmetry between the two decays. However, if the time acceptance is different for the $K^- K^+$ and $\pi^- \pi^+$ final states, a contribution from indirect CP violation remains.

The most precise measurements to date of the time-integrated CP asymmetries in $D^0 \rightarrow K^- K^+$ and $D^0 \rightarrow \pi^- \pi^+$ were made by the CDF, BABAR, and Belle collaborations [10,13,14]. The Heavy Flavor Averaging Group (HFAG) has combined time-integrated and time-dependent measurements of CP asymmetries, taking account of the different decay time acceptances, to obtain world average values for the indirect CP asymmetry of $a_{CP}^{\text{ind}} = (-0.03 \pm 0.23)\%$ and the difference in direct CP asymmetry between the final states of $\Delta a_{CP}^{\text{dir}} = (-0.42 \pm 0.27)\%$ [3].

In this Letter, we present a measurement of the difference in time-integrated CP asymmetries between $D^0 \rightarrow K^- K^+$ and $D^0 \rightarrow \pi^- \pi^+$, performed with 0.62 fb^{-1} of data collected at LHCb between March and June 2011. The flavor of the initial state (D^0 or \bar{D}^0) is tagged by requiring a $D^{*+} \rightarrow D^0 \pi_s^+$ decay, with the flavor determined by the charge of the slow pion (π_s^+). The inclusion

of charge-conjugate modes is implied throughout, except in the definition of asymmetries.

The raw asymmetry for tagged D^0 decays to a final state f is given by $A_{\text{raw}}(f)$, defined as

$$A_{\text{raw}}(f) \equiv \frac{N(D^{*+} \rightarrow D^0(f)\pi_s^+) - N(D^{*-} \rightarrow \bar{D}^0(f)\pi_s^-)}{N(D^{*+} \rightarrow D^0(f)\pi_s^+) + N(D^{*-} \rightarrow \bar{D}^0(f)\pi_s^-)}, \quad (5)$$

where $N(X)$ refers to the number of reconstructed events of decay X after background subtraction.

To first order the raw asymmetries may be written as a sum of four components, due to physics and detector effects:

$$A_{\text{raw}}(f) = A_{CP}(f) + A_D(f) + A_D(\pi_s^+) + A_P(D^{*+}). \quad (6)$$

Here, $A_D(f)$ is the asymmetry in selecting the D^0 decay into the final state f , $A_D(\pi_s^+)$ is the asymmetry in selecting the slow pion from the D^{*+} decay chain, and $A_P(D^{*+})$ is the production asymmetry for D^{*+} mesons. The asymmetries A_D and A_P are defined in the same fashion as A_{raw} . The first-order expansion is valid since the individual asymmetries are small.

For a two-body decay of a spin-0 particle to a self-conjugate final state there can be no D^0 detection asymmetry, i.e., $A_D(K^-K^+) = A_D(\pi^-\pi^+) = 0$. Moreover, $A_D(\pi_s^+)$ and $A_P(D^{*+})$ are independent of f and thus in the first-order expansion of Eq. (5) those terms cancel in the difference $A_{\text{raw}}(K^-K^+) - A_{\text{raw}}(\pi^-\pi^+)$, resulting in

$$\Delta A_{CP} = A_{\text{raw}}(K^-K^+) - A_{\text{raw}}(\pi^-\pi^+). \quad (7)$$

To minimize second-order effects that are related to the slightly different kinematic properties of the two decay modes and that do not cancel in ΔA_{CP} , the analysis is performed in bins of the relevant kinematic variables, as discussed later.

The LHCb detector is a forward spectrometer covering the pseudorapidity range $2 < \eta < 5$, and is described in detail in Ref. [15]. The Ring Imaging Cherenkov (RICH) detectors are of particular importance to this analysis, providing kaon-pion discrimination for the full range of track momenta used. The nominal downstream beam direction is aligned with the $+z$ axis, and the field direction in the LHCb dipole is such that charged particles are deflected in the horizontal (xz) plane. The field polarity was changed several times during data taking: about 60% of the data were taken with the down polarity and 40% with the other.

Selections are applied to provide samples of $D^{*+} \rightarrow D^0\pi_s^+$ candidates, with $D^0 \rightarrow K^-K^+$ or $\pi^-\pi^+$. Events are required to pass both hardware and software trigger levels. A loose D^0 selection is applied in the final state of the software trigger, and in the offline analysis only candidates that are accepted by this trigger algorithm are considered. Both the trigger and offline selections impose a variety of requirements on kinematics and decay time to

isolate the decays of interest, including requirements on the track fit quality, on the D^0 and D^{*+} vertex fit quality, on the transverse momentum ($p_T > 2 \text{ GeV}/c$) and decay time ($p_T > 100 \text{ m}$) of the D^0 candidate, on the angle between the D^0 momentum in the lab frame and its daughter momenta in the D^0 rest frame ($|\cos\theta| < 0.9$), that the D^0 trajectory points back to a primary vertex, and that the D^0 daughter tracks do not. In addition, the offline analysis exploits the capabilities of the RICH system to distinguish between pions and kaons when reconstructing the D^0 meson, with no tracks appearing as both pion and kaon candidates.

A fiducial region is implemented by imposing the requirement that the slow pion lies within the central part of the detector acceptance. This is necessary because the magnetic field bends pions of one charge to the left and those of the other charge to the right. For soft tracks at large angles in the xz plane this implies that one charge is much more likely to remain within the 300 mrad horizontal detector acceptance, thus making $A_D(\pi_s^+)$ large. Although this asymmetry is formally independent of the D^0 decay mode, it breaks the assumption that the raw asymmetries are small and it carries a risk of second-order systematic effects if the ratio of efficiencies of $D^0 \rightarrow K^-K^+$ and $D^0 \rightarrow \pi^-\pi^+$ varies in the affected region. The fiducial requirements therefore exclude edge regions in the slow pion (p_x, p) plane. Similarly, a small region of phase space in which one charge of slow pion is more likely to be swept into the beampipe region in the downstream tracking stations, and hence has reduced efficiency, is also excluded. After the implementation of the fiducial requirements about 70% of the events are retained.

The invariant mass spectra of selected K^-K^+ and $\pi^-\pi^+$ pairs are shown in Fig. 1. The half width at half maximum of the signal line shape is $8.6 \text{ MeV}/c^2$ for K^-K^+ and $11.2 \text{ MeV}/c^2$ for $\pi^-\pi^+$, where the difference is due to the kinematics of the decays and has no relevance for the subsequent analysis. The mass difference (δm) spectra of selected candidates, where $\delta m \equiv m(h^-h^+\pi_s^+) - m(h^-h^+) - m(\pi^+)$ for $h = K, \pi$, are shown in Fig. 2. Candidates are required to lie inside a wide δm window of 0–15 MeV/c^2 , and in Fig. 2 and for all subsequent results candidates are in addition required to lie in a mass signal window of 1844–1884 MeV/c^2 . The D^{*+} signal yields are approximately 1.44×10^6 in the K^-K^+ sample, and 0.38×10^6 in the $\pi^-\pi^+$ sample. Charm from b -hadron decays is strongly suppressed by the requirement that the D^0 originate from a primary vertex, and accounts for only 3% of the total yield. Of the events that contain at least one D^{*+} candidate, 12% contain more than one candidate; this is expected due to background soft pions from the primary vertex and all candidates are accepted. The background-subtracted average decay time of D^0 candidates passing the selection is measured for each final state, and the fractional difference $\Delta\langle t \rangle/\tau$ is obtained.

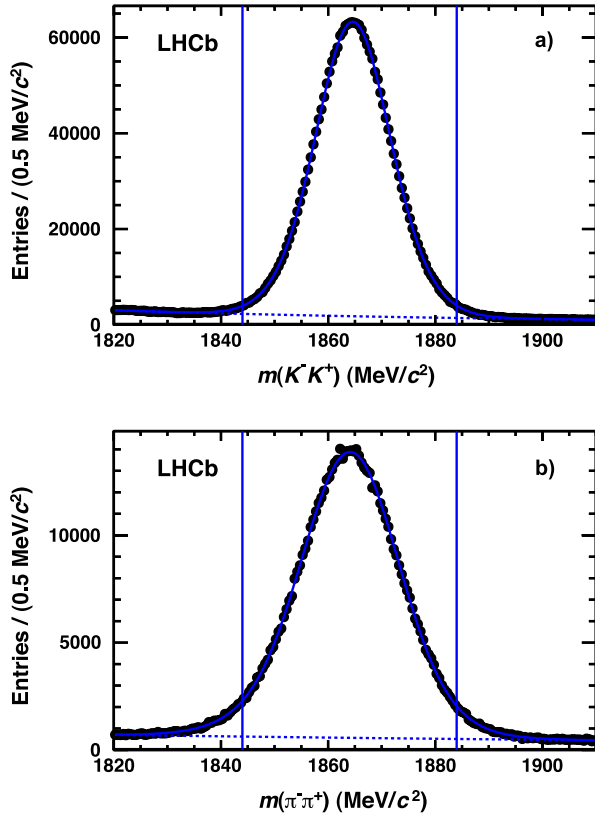


FIG. 1 (color online). Fits to the (a) $m(K^-K^+)$ and (b) $m(\pi^-\pi^+)$ spectra of D^{*+} candidates passing the selection and satisfying $0 < \delta m < 15$ MeV/ c^2 . The dashed line corresponds to the background component in the fit, and the vertical lines indicate the signal window of 1844–1884 MeV/ c^2 .

Systematic uncertainties on this quantity are assigned for the uncertainty on the world average D^0 lifetime τ (0.04%), charm from b -hadron decays (0.18%), and the background-subtraction procedure (0.04%). Combining the systematic uncertainties in quadrature, we obtain $\Delta\langle t \rangle / \tau = [9.83 \pm 0.22(\text{stat}) \pm 0.19(\text{syst})]\%$. The $\pi^-\pi^+$ and K^-K^+ average decay time is $\langle t \rangle = (0.8539 \pm 0.0005)$ ps, where the error is statistical only.

Fits are performed on the samples in order to determine $A_{\text{raw}}(K^-K^+)$ and $A_{\text{raw}}(\pi^-\pi^+)$. The production and detection asymmetries can vary with p_T and pseudorapidity η , and so can the detection efficiency of the two different D^0 decays, in particular, through the effects of the particle identification requirements. The analysis is performed in 54 kinematic bins defined by the p_T and η of the D^{*+} candidates, the momentum of the slow pion, and the sign of p_x of the slow pion at the D^{*+} vertex. The events are further partitioned in two ways. First, the data are divided between the two dipole magnet polarities. Second, the first 60% of data are processed separately from the remainder, with the division aligned with a break in data taking due to an LHC technical stop. In total, 216 statistically independent measurements are considered for each decay mode.

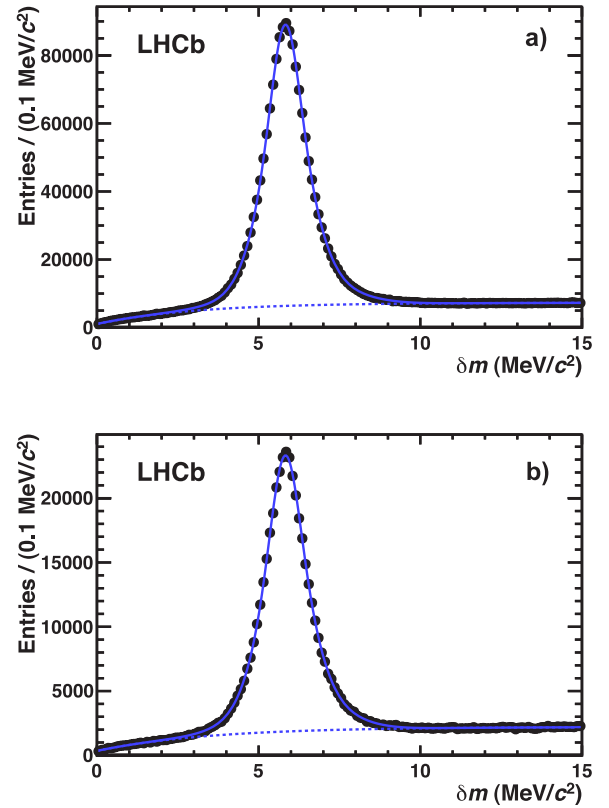


FIG. 2 (color online). Fits to the δm spectra, where the D^0 is reconstructed in the final states (a) K^-K^+ and (b) $\pi^-\pi^+$, with mass lying in the window of 1844–1884 MeV/ c^2 . The dashed line corresponds to the background component in the fit.

In each bin, one-dimensional unbinned maximum likelihood fits to the δm spectra are performed. The signal is described as the sum of two Gaussian functions with a common mean μ but different widths σ_i , convolved with a function $B(\delta m; s) = \Theta(\delta m)\delta m^s$ taking account of the asymmetric shape of the measured δm distribution. Here, $s \simeq -0.975$ is a shape parameter fixed to the value determined from the global fits shown in Fig. 2, Θ is the Heaviside step function, and the convolution runs over δm . The background is described by an empirical function of the form $1 - e^{-(\delta m - \delta m_0)/\alpha}$, where δm_0 and α are free parameters describing the threshold and shape of the function, respectively. The D^{*+} and D^{*-} samples in a given bin are fitted simultaneously and share all shape parameters, except for a charge-dependent offset in the central value μ and an overall scale factor in the mass resolution. The raw asymmetry in the signal yields is extracted directly from this simultaneous fit. No fit parameters are shared between the 216 subsamples of data, nor between the K^-K^+ and $\pi^-\pi^+$ final states.

The fits do not distinguish between the signal and backgrounds that peak in δm . Such backgrounds can arise from D^{*+} decays in which the correct slow pion is found but the

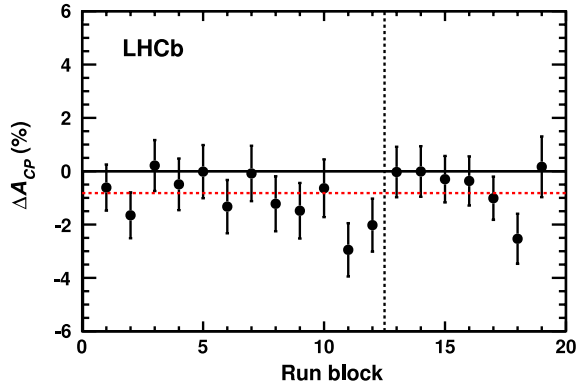


FIG. 3 (color online). Time dependence of the measurement. The data are divided into 19 disjoint, contiguous, time-ordered blocks and the value of ΔA_{CP} measured in each block. The horizontal red dashed line shows the result for the combined sample. The vertical dashed line indicates the technical stop referred to in Table I.

D^0 is partially misreconstructed. These backgrounds are suppressed by the use of tight particle identification requirements and a narrow D^0 mass window. From studies of the D^0 mass sidebands (1820–1840 and 1890–1910 MeV/c^2), this contamination is found to be approximately 1% of the signal yield and to have small raw asymmetry (consistent with zero asymmetry difference between the $K^- K^+$ and $\pi^- \pi^+$ final states). Its effect on the measurement is estimated in an ensemble of simulated experiments and found to be negligible; a systematic uncertainty is assigned below based on the statistical precision of the estimate.

A value of ΔA_{CP} is determined in each measurement bin as the difference between $A_{\text{raw}}(K^- K^+)$ and $A_{\text{raw}}(\pi^- \pi^+)$. Testing these 216 measurements for mutual consistency, we obtain $\chi^2/\text{ndf} = 211/215$ (χ^2 probability of 56%). A

TABLE I. Values of ΔA_{CP} measured in subsamples of the data, and the χ^2/ndf and corresponding χ^2 probabilities for internal consistency among the 27 bins in each subsample. The data are divided before and after a technical stop (TS), by magnet polarity (up, down), and by the sign of p_x for the slow pion (left, right). The consistency among the eight subsamples is $\chi^2/\text{ndf} = 6.8/7$ (45%).

Subsample	$\Delta A_{CP}[\%]$	χ^2/ndf
Pre-TS, up, left	-1.22 ± 0.59	13/26(98%)
Pre-TS, up, right	-1.43 ± 0.59	27/26(39%)
Pre-TS, down, left	-0.59 ± 0.52	19/26(84%)
Pre-TS, down, right	-0.51 ± 0.52	29/26(30%)
Post-TS, up, left	-0.79 ± 0.90	26/26(44%)
Post-TS, up, right	$+0.42 \pm 0.93$	21/26(77%)
Post-TS, down, left	-0.24 ± 0.56	34/26(15%)
Post-TS, down, right	-1.59 ± 0.57	35/26(12%)
All data	-0.82 ± 0.21	211/215(56%)

weighted average is performed to yield the result $\Delta A_{CP} = (-0.82 \pm 0.21)\%$, where the uncertainty is statistical only.

Numerous robustness checks are made. The value of ΔA_{CP} is studied as a function of the time at which the data were taken (Fig. 3) and found to be consistent with a constant value (χ^2 probability of 57%). The measurement is repeated with progressively more restrictive RICH particle identification requirements, finding values of $(-0.88 \pm 0.26)\%$ and $(-1.03 \pm 0.31)\%$; both of these values are consistent with the baseline result when correlations are taken into account. Table I lists ΔA_{CP} for eight disjoint subsamples of data split according to magnet polarity, the sign of p_x of the slow pion, and whether the data were taken before or after the technical stop. The χ^2 probability for consistency among the subsamples is 45%. The significances of the differences between data taken before and after the technical stop, between the magnet polarities, and between $p_x > 0$ and $p_x < 0$ are 0.4, 0.6, and 0.7 standard deviations, respectively. Other checks include applying electron and muon vetoes to the slow pion and to the D^0 daughters, use of different kinematic binnings, validation of the size of the statistical uncertainties with Monte Carlo pseudoexperiments, tightening of kinematic requirements, testing for variation of the result with the multiplicity of tracks and of primary vertices in the event, use of other signal and background parameterizations in the fit, and imposing a full set of common shape parameters between D^{*+} and D^{*-} candidates. Potential biases due to the inclusive hardware trigger selection are investigated with the subsample of data in which one of the signal final-state tracks is directly responsible for the hardware trigger decision. In all cases good stability is observed. For several of these checks, a reduced number of kinematic bins are used for simplicity. No systematic dependence of ΔA_{CP} is observed with respect to the kinematic variables.

Systematic uncertainties are assigned by loosening the fiducial requirement on the slow pion, assessing the effect of potential peaking backgrounds in Monte Carlo pseudoexperiments, repeating the analysis with the asymmetry extracted through sideband subtraction in δm instead of a fit, removing all candidates but one (chosen at random) in events with multiple candidates, and comparing with the result obtained without kinematic binning. In each case the

TABLE II. Summary of absolute systematic uncertainties for ΔA_{CP} .

Source	Uncertainty
Fiducial requirement	0.01%
Peaking background asymmetry	0.04%
Fit procedure	0.08%
Multiple candidates	0.06%
Kinematic binning	0.02%
Total	0.11%

full value of the change in result is taken as the systematic uncertainty. These uncertainties are listed in Table II. The sum in quadrature is 0.11%. Combining statistical and systematic uncertainties in quadrature, this result is consistent at the 1σ level with the current HFAG world average [3].

In conclusion, the time-integrated difference in CP asymmetry between $D^0 \rightarrow K^- K^+$ and $D^0 \rightarrow \pi^- \pi^+$ decays has been measured to be

$$\Delta A_{CP} = [-0.82 \pm 0.21(\text{stat}) \pm 0.11(\text{syst})]\%$$

with 0.62 fb^{-1} of 2011 data. Given the dependence of ΔA_{CP} on the direct and indirect CP asymmetries, shown in Eq. (4), and the measured value $\Delta\langle t \rangle/\tau = [9.83 \pm 0.22(\text{stat}) \pm 0.19(\text{syst})]\%$, the contribution from indirect CP violation is suppressed and ΔA_{CP} is primarily sensitive to direct CP violation. Dividing the central value by the sum in quadrature of the statistical and systematic uncertainties, the significance of the measured deviation from zero is 3.5σ . This is the first evidence for CP violation in the charm sector. To establish whether this result is consistent with the SM will require the analysis of more data, as well as improved theoretical understanding.

We express our gratitude to our colleagues in the CERN accelerator departments for the excellent performance of the LHC. We thank the technical and administrative staff at CERN and at the LHCb institutes, and acknowledge support from the National Agencies: CAPES, CNPq, FAPERJ and FINEP (Brazil); CERN; NSFC (China); CNRS/IN2P3 (France); BMBF, DFG, HGF and MPG (Germany); SFI (Ireland); INFN (Italy); FOM and NWO (The Netherlands); SCSR (Poland); ANCS (Romania); MinES of Russia and Rosatom (Russia); MICINN, XuntaGal and

GENCAT (Spain); SNSF and SER (Switzerland); NAS Ukraine (Ukraine); STFC (United Kingdom); NSF (USA). We also acknowledge the support received from the ERC under FP7 and the Region Auvergne.

-
- [1] B. Aubert *et al.* (BABAR Collaboration), *Phys. Rev. Lett.* **98**, 211802 (2007).
 - [2] M. Staric *et al.* (Belle Collaboration), *Phys. Rev. Lett.* **98**, 211803 (2007).
 - [3] D. Asner *et al.* (Heavy Flavor Averaging Group), [arXiv:1010.1589](https://arxiv.org/abs/1010.1589).
 - [4] A.F. Falk, Y. Grossman, Z. Ligeti, Y. Nir, and A.A. Petrov, *Phys. Rev. D* **69**, 114021 (2004).
 - [5] Y. Grossman, A.L. Kagan, and Y. Nir, *Phys. Rev. D* **75**, 036008 (2007).
 - [6] S. Bianco, F.L. Fabbri, D. Benson, and I. Bigi, *Riv. Nuovo Cimento* **26**, 1 (2003).
 - [7] M. Bobrowski, A. Lenz, J. Riedl, and J. Rohrwild, *J. High Energy Phys.* **03** (2010) 009.
 - [8] A.A. Petrov, PoS, BEAUTY2009 (2009) 024.
 - [9] I.I. Bigi, M. Blanke, A.J. Buras, and S. Recksiegel, *J. High Energy Phys.* **07** (2009) 097.
 - [10] T. Aaltonen *et al.* (CDF Collaboration) *Phys. Rev. D* **85**, 012009 (2012).
 - [11] I.I. Bigi, A. Paul, and S. Recksiegel, *J. High Energy Phys.* **06** (2011) 089.
 - [12] A.L. Kagan and M.D. Sokoloff, *Phys. Rev. D* **80**, 076008 (2009).
 - [13] B. Aubert *et al.* (BABAR Collaboration), *Phys. Rev. Lett.* **100**, 061803 (2008).
 - [14] M. Staric *et al.* (Belle Collaboration), *Phys. Lett. B* **670**, 190 (2008).
 - [15] A. A. Alves, Jr *et al.* (LHCb Collaboration), *JINST* **3**, S08005 (2008).

R. Aaij,²³ C. Abellan Beteta,^{35,n} B. Adeva,³⁶ M. Adinolfi,⁴² C. Adrover,⁶ A. Affolder,⁴⁸ Z. Ajaltouni,⁵ J. Albrecht,³⁷ F. Alessio,³⁷ M. Alexander,⁴⁷ G. Alkhalazov,²⁹ P. Alvarez Cartelle,³⁶ A. A. Alves Jr,²² S. Amato,² Y. Amhis,³⁸ J. Anderson,³⁹ R. B. Appleby,⁵⁰ O. Aquines Gutierrez,¹⁰ F. Archilli,^{18,37} L. Arrabito,⁵³ A. Artamonov,³⁴ M. Artuso,^{52,37} E. Aslanides,⁶ G. Auriemma,^{22,m} S. Bachmann,¹¹ J.J. Back,⁴⁴ D.S. Bailey,⁵⁰ V. Balagura,^{30,37} W. Baldini,¹⁶ R.J. Barlow,⁵⁰ C. Barschel,³⁷ S. Barsuk,⁷ W. Barter,⁴³ A. Bates,⁴⁷ C. Bauer,¹⁰ Th. Bauer,²³ A. Bay,³⁸ I. Bediaga,¹ S. Belogurov,³⁰ K. Belous,³⁴ I. Belyaev,^{30,37} E. Ben-Haim,⁸ M. Benayoun,⁸ G. Bencivenni,¹⁸ S. Benson,⁴⁶ J. Benton,⁴² R. Bernet,³⁹ M.-O. Bettler,¹⁷ M. van Beuzekom,²³ A. Bien,¹¹ S. Bifani,¹² T. Bird,⁵⁰ A. Bizzeti,^{17,h} P.M. Bjørnstad,⁵⁰ T. Blake,³⁷ F. Blanc,³⁸ C. Blanks,⁴⁹ J. Blouw,¹¹ S. Blusk,⁵² A. Bobrov,³³ V. Bocci,²² A. Bondar,³³ N. Bondar,²⁹ W. Bonivento,¹⁵ S. Borghi,^{47,50} A. Borgia,⁵² T. J. V. Bowcock,⁴⁸ C. Bozzi,¹⁶ T. Brambach,⁹ J. van den Brand,²⁴ J. Bressieux,³⁸ D. Brett,⁵⁰ M. Britsch,¹⁰ T. Britton,⁵² N.H. Brook,⁴² H. Brown,⁴⁸ A. Büchler-Germann,³⁹ I. Burducea,²⁸ A. Bursche,³⁹ J. Buytaert,³⁷ S. Cadeddu,¹⁵ O. Callot,⁷ M. Calvi,^{20,j} M. Calvo Gomez,^{35,n} A. Camboni,³⁵ P. Campana,^{18,37} A. Carbone,¹⁴ G. Carboni,^{21,k} R. Cardinale,^{19,37,i} A. Cardini,¹⁵ L. Carson,⁴⁹ K. Carvalho Akiba,² G. Casse,⁴⁸ M. Cattaneo,³⁷ Ch. Cauet,⁹ M. Charles,⁵¹ Ph. Charpentier,³⁷ N. Chiapolini,³⁹ K. Ciba,³⁷ X. Cid Vidal,³⁶ G. Ciezarek,⁴⁹ P.E.L. Clarke,^{46,37} M. Clemencic,³⁷ H.V. Cliff,⁴³ J. Closier,³⁷ C. Coca,²⁸ V. Coco,²³ J. Cogan,⁶ P. Collins,³⁷ A. Comerma-Montells,³⁵ F. Constantin,²⁸ A. Contu,⁵¹ A. Cook,⁴² M. Coombes,⁴² G. Corti,³⁷ G.A. Cowan,³⁸ R. Currie,⁴⁶ C. D'Ambrosio,³⁷ P. David,⁸ P.N.Y. David,²³ I. De Bonis,⁴ S. De Capua,^{21,k} M. De Cian,³⁹ F. De Lorenzi,¹² J.M. De Miranda,¹ L. De Paula,² P. De Simone,¹⁸ D. Decamp,⁴ M. Deckenhoff,⁹ H. Degaudenzi,^{38,37} L. Del Buono,⁸ C. Deplano,¹⁵ D. Derkach,^{14,37} O. Deschamps,⁵

F. Dettori,²⁴ J. Dickens,⁴³ H. Dijkstra,³⁷ P. Diniz Batista,¹ F. Domingo Bonal,^{35,n} S. Donleavy,⁴⁸ F. Dordei,¹¹ A. Dosil Suárez,³⁶ D. Dossett,⁴⁴ A. Dovbnaya,⁴⁰ F. Dupertuis,³⁸ R. Dzhelyadin,³⁴ A. Dziurda,²⁵ S. Easo,⁴⁵ U. Egede,⁴⁹ V. Egorychev,³⁰ S. Eidelman,³³ D. van Eijk,²³ F. Eisele,¹¹ S. Eisenhardt,⁴⁶ R. Ekelhof,⁹ L. Eklund,⁴⁷ Ch. Elsasser,³⁹ D. Elsby,⁵⁵ D. Esperante Pereira,³⁶ L. Estève,⁴³ A. Falabella,^{16,14,e} E. Fanchini,^{20,j} C. Färber,¹¹ G. Fardell,⁴⁶ C. Farinelli,²³ S. Farry,¹² V. Fave,³⁸ V. Fernandez Albor,³⁶ M. Ferro-Luzzi,³⁷ S. Filippov,³² C. Fitzpatrick,⁴⁶ M. Fontana,¹⁰ F. Fontanelli,^{19,i} R. Forty,³⁷ M. Frank,³⁷ C. Frei,³⁷ M. Frosini,^{17,37,f} S. Furcas,²⁰ A. Gallas Torreira,³⁶ D. Galli,^{14,c} M. Gandelman,² P. Gandini,⁵¹ Y. Gao,³ J.-C. Garnier,³⁷ J. Garofoli,⁵² J. Garra Tico,⁴³ L. Garrido,³⁵ D. Gascon,³⁵ C. Gaspar,³⁷ N. Gauvin,³⁸ M. Gersabeck,³⁷ T. Gershon,^{44,37} Ph. Ghez,⁴ V. Gibson,⁴³ V. V. Gligorov,³⁷ C. Göbel,⁵⁴ D. Golubkov,³⁰ A. Golutvin,^{49,30,37} A. Gomes,² H. Gordon,⁵¹ M. Grabalosa Gándara,³⁵ R. Graciani Diaz,³⁵ L. A. Granado Cardoso,³⁷ E. Graugés,³⁵ G. Graziani,¹⁷ A. Grecu,²⁸ E. Greening,⁵¹ S. Gregson,⁴³ B. Gui,⁵² E. Gushchin,³² Yu. Guz,³⁴ T. Gys,³⁷ G. Haefeli,³⁸ C. Haen,³⁷ S. C. Haines,⁴³ T. Hampson,⁴² S. Hansmann-Menzemer,¹¹ R. Harji,⁴⁹ N. Harnew,⁵¹ J. Harrison,⁵⁰ P. F. Harrison,⁴⁴ T. Hartmann,⁵⁶ J. He,⁷ V. Heijne,²³ K. Hennessy,⁴⁸ P. Henrard,⁵ J. A. Hernando Morata,³⁶ E. van Herwijnen,³⁷ E. Hicks,⁴⁸ K. Holubyev,¹¹ P. Hopchev,⁴ W. Hulsbergen,²³ P. Hunt,⁵¹ T. Huse,⁴⁸ R. S. Huston,¹² D. Hutchcroft,⁴⁸ D. Hynds,⁴⁷ V. Iakovenko,⁴¹ P. Ilten,¹² J. Imong,⁴² R. Jacobsson,³⁷ A. Jaeger,¹¹ M. Jahjah Hussein,⁵ E. Jans,²³ F. Jansen,²³ P. Jatou,³⁸ B. Jean-Marie,⁷ F. Jing,³ M. John,⁵¹ D. Johnson,⁵¹ C. R. Jones,⁴³ B. Jost,³⁷ M. Kabbalo,⁹ S. Kandybei,⁴⁰ M. Karacson,³⁷ T. M. Karbach,⁹ J. Keaveney,¹² I. R. Kenyon,⁵⁵ U. Kerzel,³⁷ T. Ketel,²⁴ A. Keune,³⁸ B. Khanji,⁶ Y. M. Kim,⁴⁶ M. Knecht,³⁸ R. Koopman,²⁴ P. Koppenburg,²³ A. Kozlinskiy,²³ L. Kravchuk,³² K. Kreplin,¹¹ M. Krepis,⁴⁴ G. Krocker,¹¹ P. Krokovny,¹¹ F. Kruse,⁹ K. Kruzelecki,³⁷ M. Kucharczyk,^{20,25,37,j} T. Kvaratskheliya,^{30,37} V. N. La Thi,³⁸ D. Lacarrere,³⁷ G. Lafferty,⁵⁰ A. Lai,¹⁵ D. Lambert,⁴⁶ R. W. Lambert,²⁴ E. Lanciotti,³⁷ G. Lanfranchi,¹⁸ C. Langenbruch,¹¹ T. Latham,⁴⁴ C. Lazzeroni,⁵⁵ R. Le Gac,⁶ J. van Leerdam,²³ J.-P. Lees,⁴ R. Lefèvre,⁵ A. Leflat,^{31,37} J. Lefrançois,⁷ O. Leroy,⁶ T. Lesiak,²⁵ L. Li,³ L. Li Gioi,⁵ M. Lieng,⁹ M. Liles,⁴⁸ R. Lindner,³⁷ C. Linn,¹¹ B. Liu,³ G. Liu,³⁷ J. von Loeben,²⁰ J. H. Lopes,² E. Lopez Asamar,³⁵ N. Lopez-March,³⁸ H. Lu,^{38,3} J. Luisier,³⁸ A. Mac Raighne,⁴⁷ F. Machefert,⁷ I. V. Machikhiliyan,^{4,30} F. Maciuc,¹⁰ O. Maev,^{29,37} J. Magnin,¹ S. Malde,⁵¹ R. M. D. Mamunur,³⁷ G. Manca,^{15,d} G. Mancinelli,⁶ N. Mangiafave,⁴³ U. Marconi,¹⁴ R. Märki,³⁸ J. Marks,¹¹ G. Martellotti,²² A. Martens,⁸ L. Martin,⁵¹ A. Martín Sánchez,⁷ D. Martinez Santos,³⁷ A. Massafferri,¹ Z. Mathe,¹² C. Matteuzzi,²⁰ M. Matveev,²⁹ E. Maurice,⁶ B. Maynard,⁵² A. Mazurov,^{16,32,37} G. McGregor,⁵⁰ R. McNulty,¹² M. Meissner,¹¹ M. Merk,²³ J. Merkel,⁹ R. Messi,^{21,k} S. Miglioranzì,³⁷ D. A. Milanes,^{13,37} M.-N. Minard,⁴ J. Molina Rodriguez,⁵⁴ S. Monteil,⁵ D. Moran,¹² P. Morawski,²⁵ R. Mountain,⁵² I. Mous,²³ F. Muheim,⁴⁶ K. Müller,³⁹ R. Muresan,^{28,38} B. Muryn,²⁶ B. Muster,³⁸ M. Musy,³⁵ J. Mylroie-Smith,⁴⁸ P. Naik,⁴² T. Nakada,³⁸ R. Nandakumar,⁴⁵ I. Nasteva,¹ M. Nedos,⁹ M. Needham,⁴⁶ N. Neufeld,³⁷ C. Nguyen-Mau,^{38,o} M. Nicol,⁷ V. Niess,⁵ N. Nikitin,³¹ A. Nomerotski,⁵¹ A. Novoselov,³⁴ A. Oblakowska-Mucha,²⁶ V. Obraztsov,³⁴ S. Oggero,²³ S. Ogilvy,⁴⁷ O. Okhrimenko,⁴¹ R. Oldeman,^{15,d} M. Orlandea,²⁸ J. M. Otalora Goicochea,² P. Owen,⁴⁹ K. Pal,⁵² J. Palacios,³⁹ A. Palano,^{13,b} M. Palutan,¹⁸ J. Panman,³⁷ A. Papanestis,⁴⁵ M. Pappagallo,⁴⁷ C. Parkes,^{50,37} C. J. Parkinson,⁴⁹ G. Passaleva,¹⁷ G. D. Patel,⁴⁸ M. Patel,⁴⁹ S. K. Paterson,⁴⁹ G. N. Patrick,⁴⁵ C. Patrignani,^{19,i} C. Pavel-Nicorescu,²⁸ A. Pazos Alvarez,³⁶ A. Pellegrino,²³ G. Penso,^{22,1} M. Pepe Altarelli,³⁷ S. Perazzini,^{14,c} D. L. Perego,^{20,j} E. Perez Trigo,³⁶ A. Pérez-Calero Yzquierdo,³⁵ P. Perret,⁵ M. Perrin-Terrin,⁶ G. Pessina,²⁰ A. Petrella,^{16,37} A. Petrolini,^{19,i} A. Phan,⁵² E. Picatoste Olloqui,³⁵ B. Pie Valls,³⁵ B. Pietrzyk,⁴ T. Pilař,⁴⁴ D. Pinci,²² R. Plackett,⁴⁷ S. Playfer,⁴⁶ M. Plo Casasus,³⁶ G. Polok,²⁵ A. Poluektov,^{44,33} E. Polycarpo,² D. Popov,¹⁰ B. Popovici,²⁸ C. Potterat,³⁵ A. Powell,⁵¹ J. Prisciandaro,³⁸ V. Pugatch,⁴¹ A. Puig Navarro,³⁵ W. Qian,⁵² J. H. Rademacker,⁴² B. Rakotomiramanana,³⁸ M. S. Rangel,² I. Raniuk,⁴⁰ G. Raven,²⁴ S. Redford,⁵¹ M. M. Reid,⁴⁴ A. C. dos Reis,¹ S. Ricciardi,⁴⁵ K. Rinnert,⁴⁸ D. A. Roa Romero,⁵ P. Robbe,⁷ E. Rodrigues,^{47,50} F. Rodrigues,² P. Rodriguez Perez,³⁶ G. J. Rogers,⁴³ S. Roiser,³⁷ V. Romanovsky,³⁴ M. Rosello,^{35,n} J. Rouvinet,³⁸ T. Ruf,³⁷ H. Ruiz,³⁵ G. Sabatino,^{21,k} J. J. Saborido Silva,³⁶ N. Sagidova,²⁹ P. Sail,⁴⁷ B. Saitta,^{15,d} C. Salzmann,³⁹ M. Sannino,^{19,i} R. Santacesaria,²² C. Santamarina Rios,³⁶ R. Santinelli,³⁷ E. Santovetti,^{21,k} M. Sapunov,⁶ A. Sarti,^{18,l} C. Satriano,^{22,m} A. Satta,²¹ M. Savrie,^{16,e} D. Savrina,³⁰ P. Schaack,⁴⁹ M. Schiller,²⁴ S. Schleich,⁹ M. Schlupp,⁹ M. Schmelling,¹⁰ B. Schmidt,³⁷ O. Schneider,³⁸ A. Schopper,³⁷ M.-H. Schune,⁷ R. Schwemmer,³⁷ B. Sciascia,¹⁸ A. Sciubba,^{18,l} M. Seco,³⁶ A. Semennikov,³⁰ K. Senderowska,²⁶ I. Sepp,⁴⁹ N. Serra,³⁹ J. Serrano,⁶ P. Seyfert,¹¹ M. Shapkin,³⁴ I. Shapoval,^{40,37} P. Shatalov,³⁰ Y. Shcheglov,²⁹ T. Shears,⁴⁸ L. Shekhtman,³³ O. Shevchenko,⁴⁰ V. Shevchenko,³⁰ A. Shires,⁴⁹ R. Silva Coutinho,⁴⁴ T. Skwarnicki,⁵² A. C. Smith,³⁷ N. A. Smith,⁴⁸ E. Smith,^{51,45} K. Sobczak,⁵ F. J. P. Soler,⁴⁷ A. Solomin,⁴² F. Soomro,¹⁸ B. Souza De Paula,² B. Spaan,⁹ A. Sparkes,⁴⁶ P. Spradlin,⁴⁷ F. Stagni,³⁷ S. Stahl,¹¹

O. Steinkamp,³⁹ S. Stoica,²⁸ S. Stone,^{52,37} B. Storaci,²³ M. Straticiu,²⁸ U. Straumann,³⁹ V. K. Subbiah,³⁷ S. Swientek,⁹ M. Szczekowski,²⁷ P. Szczypka,³⁸ T. Szumlak,²⁶ S. T'Jampens,⁴ E. Teodorescu,²⁸ F. Teubert,³⁷ C. Thomas,⁵¹ E. Thomas,³⁷ J. van Tilburg,¹¹ V. Tisserand,⁴ M. Tobin,³⁹ S. Topp-Joergensen,⁵¹ N. Torr,⁵¹ E. Tournefier,^{4,49} M. T. Tran,³⁸ A. Tsaregorodtsev,⁶ N. Tuning,²³ M. Ubeda Garcia,³⁷ A. Ukleja,²⁷ P. Urquijo,⁵² U. Uwer,¹¹ V. Vagnoni,¹⁴ G. Valenti,¹⁴ R. Vazquez Gomez,³⁵ P. Vazquez Regueiro,³⁶ S. Vecchi,¹⁶ J. J. Velthuis,⁴² M. Veltri,^{17,g} B. Viaud,⁷ I. Videau,⁷ X. Vilasis-Cardona,^{35,n} J. Visniakov,³⁶ A. Vollhardt,³⁹ D. Volyansky,¹⁰ D. Voong,⁴² A. Vorobyev,²⁹ H. Voss,¹⁰ S. Wandernoth,¹¹ J. Wang,⁵² D. R. Ward,⁴³ N. K. Watson,⁵⁵ A. D. Webber,⁵⁰ D. Websdale,⁴⁹ M. Whitehead,⁴⁴ D. Wiedner,¹¹ L. Wiggers,²³ G. Wilkinson,⁵¹ M. P. Williams,^{44,45} M. Williams,⁴⁹ F. F. Wilson,⁴⁵ J. Wishahi,⁹ M. Witek,²⁵ W. Witzeling,³⁷ S. A. Wotton,⁴³ K. Wyllie,³⁷ Y. Xie,⁴⁶ F. Xing,⁵¹ Z. Xing,⁵² Z. Yang,³ R. Young,⁴⁶ O. Yushchenko,³⁴ M. Zavertyaev,^{10,a} F. Zhang,³ L. Zhang,⁵² W. C. Zhang,¹² Y. Zhang,³ A. Zhelezov,¹¹ L. Zhong,³ E. Zverev,³¹ and A. Zvyagin³⁷

(LHCb Collaboration)

¹Centro Brasileiro de Pesquisas Físicas (CBPF), Rio de Janeiro, Brazil

²Universidade Federal do Rio de Janeiro (UFRJ), Rio de Janeiro, Brazil

³Center for High Energy Physics, Tsinghua University, Beijing, China

⁴LAPP, Université de Savoie, CNRS/IN2P3, Annecy-Le-Vieux, France

⁵Clermont Université, Université Blaise Pascal, CNRS/IN2P3, LPC, Clermont-Ferrand, France

⁶CPPM, Aix-Marseille Université, CNRS/IN2P3, Marseille, France

⁷LAL, Université Paris-Sud, CNRS/IN2P3, Orsay, France

⁸LPNHE, Université Pierre et Marie Curie, Université Paris Diderot, CNRS/IN2P3, Paris, France

⁹Fakultät Physik, Technische Universität Dortmund, Dortmund, Germany

¹⁰Max-Planck-Institut für Kernphysik (MPIK), Heidelberg, Germany

¹¹Physikalisches Institut, Ruprecht-Karls-Universität Heidelberg, Heidelberg, Germany

¹²School of Physics, University College Dublin, Dublin, Ireland

¹³Sezione INFN di Bari, Bari, Italy

¹⁴Sezione INFN di Bologna, Bologna, Italy

¹⁵Sezione INFN di Cagliari, Cagliari, Italy

¹⁶Sezione INFN di Ferrara, Ferrara, Italy

¹⁷Sezione INFN di Firenze, Firenze, Italy

¹⁸Laboratori Nazionali dell'INFN di Frascati, Frascati, Italy

¹⁹Sezione INFN di Genova, Genova, Italy

²⁰Sezione INFN di Milano Bicocca, Milano, Italy

²¹Sezione INFN di Roma Tor Vergata, Roma, Italy

²²Sezione INFN di Roma La Sapienza, Roma, Italy

²³Nikhef National Institute for Subatomic Physics, Amsterdam, The Netherlands

²⁴Nikhef National Institute for Subatomic Physics and Vrije Universiteit, Amsterdam, The Netherlands

²⁵Henryk Niewodniczanski Institute of Nuclear Physics Polish Academy of Sciences, Kraków, Poland

²⁶AGH University of Science and Technology, Kraków, Poland

²⁷Soltan Institute for Nuclear Studies, Warsaw, Poland

²⁸Horia Hulubei National Institute of Physics and Nuclear Engineering, Bucharest-Magurele, Romania

²⁹Petersburg Nuclear Physics Institute (PNPI), Gatchina, Russia

³⁰Institute of Theoretical and Experimental Physics (ITEP), Moscow, Russia

³¹Institute of Nuclear Physics, Moscow State University (SINP MSU), Moscow, Russia

³²Institute for Nuclear Research of the Russian Academy of Sciences (INR RAN), Moscow, Russia

³³Budker Institute of Nuclear Physics (SB RAS) and Novosibirsk State University, Novosibirsk, Russia

³⁴Institute for High Energy Physics (IHEP), Protvino, Russia

³⁵Universitat de Barcelona, Barcelona, Spain

³⁶Universidad de Santiago de Compostela, Santiago de Compostela, Spain

³⁷European Organization for Nuclear Research (CERN), Geneva, Switzerland

³⁸Ecole Polytechnique Fédérale de Lausanne (EPFL), Lausanne, Switzerland

³⁹Physik-Institut, Universität Zürich, Zürich, Switzerland

⁴⁰NSC Kharkiv Institute of Physics and Technology (NSC KIPT), Kharkiv, Ukraine

⁴¹Institute for Nuclear Research of the National Academy of Sciences (KINR), Kyiv, Ukraine

⁴²H.H. Wills Physics Laboratory, University of Bristol, Bristol, United Kingdom

⁴³Cavendish Laboratory, University of Cambridge, Cambridge, United Kingdom

⁴⁴Department of Physics, University of Warwick, Coventry, United Kingdom

- ⁴⁵*STFC Rutherford Appleton Laboratory, Didcot, United Kingdom*
⁴⁶*School of Physics and Astronomy, University of Edinburgh, Edinburgh, United Kingdom*
⁴⁷*School of Physics and Astronomy, University of Glasgow, Glasgow, United Kingdom*
⁴⁸*Oliver Lodge Laboratory, University of Liverpool, Liverpool, United Kingdom*
⁴⁹*Imperial College London, London, United Kingdom*
⁵⁰*School of Physics and Astronomy, University of Manchester, Manchester, United Kingdom*
⁵¹*Department of Physics, University of Oxford, Oxford, United Kingdom*
⁵²*Syracuse University, Syracuse, New York, USA*
⁵³*CC-IN2P3, CNRS/IN2P3, Lyon-Villeurbanne, France*
⁵⁴*Pontifícia Universidade Católica do Rio de Janeiro (PUC-Rio), Rio de Janeiro, Brazil*
⁵⁵*University of Birmingham, Birmingham, United Kingdom*
⁵⁶*Physikalisches Institut, Universität Rostock, Rostock, Germany*

^aAlso at P.N. Lebedev Physical Institute, Russian Academy of Science (LPI RAS), Moscow, Russia.

^bAlso at Università di Bari, Bari, Italy.

^cAlso at Università di Bologna, Bologna, Italy.

^dAlso at Università di Cagliari, Cagliari, Italy.

^eAlso at Università di Ferrara, Ferrara, Italy.

^fAlso at Università di Firenze, Firenze, Italy.

^gAlso at Università di Urbino, Urbino, Italy.

^hAlso at Università di Modena e Reggio Emilia, Modena, Italy.

ⁱAlso at Università di Genova, Genova, Italy.

^jAlso at Università di Milano Bicocca, Milano, Italy.

^kAlso at Università di Roma Tor Vergata, Roma, Italy.

^lAlso at Università di Roma La Sapienza, Roma, Italy.

^mAlso at Università della Basilicata, Potenza, Italy.

ⁿAlso at LIFAELS, La Salle, Universitat Ramon Llull, Barcelona, Spain.

^oAlso at Hanoi University of Science, Hanoi, Vietnam.